

Comments on "Robust reversible data hiding scheme based on two-layer embedding strategy"

Wen Yin^a, Longfei Ke^a, Zhaoxia Yin^{a,*}, Jin Tang^a and Bin Luo^a

^a*Anhui Province Key Laboratory of Multimodal Cognitive Computation, School of Computer Science and Technology, Anhui University, 230601, P.R.China*

ARTICLE INFO

Keywords:
 Robustness
 Reversible data hiding
 Least significant bit
 Prediction error expansion
 Steganography

ABSTRACT

In paper "Robust reversible data hiding scheme based on two-layer embedding strategy" published in INS recently, Kumar et al. proposed an Robust Reversible Data Hiding (RRDH) scheme based on two-layer embedding. Secret data is embedded into Most Significant Bit (MSB) planes and sorting strategy based on local complexity is adopted to reduce distortion. However, Kumar et al.'s RDH scheme is not as robust as stated and can not be called RRDH. In this comment, we give a brief description of Kumar et al.'s RDH scheme at first and then show robust testing experiments by analysing the changes in each bit plane after Joint Photographic Experts Group (JPEG) compression and the changes in pixel value ordering.

1. Introduction

For some sensitive scenarios such as medical and military images, lossless recovery of original images and accurate extraction of the hidden data are necessary. To solve this issue, Reversible Data Hiding (RDH) is proposed to losslessly recover both the original image and the hidden data [1]. The RDH technique reversibly embeds additional data into the original image to obtain a marked image. However, in some applications, the marked image may be damaged irreversibly by lossy operations, such as JPEG compression. The hidden data can still be extracted correctly from the damaged image, even though the original image cannot be recovered reversibly, which is called RRDH [1].

The first RRDH scheme was proposed by De Vleeschouwer et al. [2], which proposed the histogram rotation technique. Their scheme suffered from salt-and-pepper noise because of modulo-256 addition, resulting in poor image quality after embedding a watermarking. To avoid the salt-and-pepper noise in [2], Ni et al. [3] proposed an RRDH scheme using a robust statistical quantity in the spatial domain to embed data and adopting error correction coding to achieve reversibility. Zeng et al. [4] extended Ni et al.'s scheme, choosing the arithmetic difference of block as robust features and embedding secret data by introducing two thresholds (T, G) and a new histogram modification scheme, which improved the robustness of the scheme. In [5], Gao et al. improve Zeng et al.'s scheme by using the statistical quantity histogram to improve the embedding capacity and robustness. The RRDH scheme has also been developed in wavelet domains. Zou et al. [6] developed a robust digital watermarking system based on shifting the absolute mean values of integer wavelet transform coefficients. Later, An et al. [7] [8] proposed a pragmatic framework called wavelet-domain statistical quantity histogram shifting and clustering, which collects the coefficients of the transformed image to produce the histogram. Coltuc et al. [9] [10] proposed a two-stage framework for RRDH. The watermarking is embedded into the original image in the robust embedding stage to generate an intermediate image. In the reversible embedding stage, the information used to reversibly recover original image is embedded into the intermediate image to generate the marked image. Because both the robust embedding stage and reversible embedding stage are operated on the same embedding domain, the watermarking extraction may be failed. To address this problem, Wang et al. [11] proposed an independent embedding domain scheme to preserve the robustness, one for robust watermarking, and the other for reversible embedding, which improved the performance of Coltuc et al.'s scheme. Xiong et al. [12] proposed an RRDH scheme with the patchwork robust watermarking and prediction error expansion based reversible watermarking to embed the watermarking exploiting the two-stage architecture. Their scheme can also preserve privacy of the original image and is suitable for multiparty copyright protection.

Recently, Wang et al. [13] proposed a lossless robust data hiding scheme based on significant-bit-difference expansion, which embedded secret data into higher significant bit planes of the image to improve the embedding capacity.

*Corresponding author. yinzhaoxia@ahu.edu.cn (Z. Yin)
 ORCID(s): 0000-0003-0387-4806 (Z. Yin)

Inspired by the work of [13], Kumar et al. [14] first decompose the original image into two planes, MSB (Here MSB is equivalent to HSB in [14], but since the more general term is MSB, we use MSB instead.) planes and Least Significant Bit (LSB) planes. Then, the MSB planes of the original image are used to embed secret data by making a prediction error expansion with two-layer embedding. In this way, Kumar et al. achieve the robustness of their scheme against minor modification attacks like JPEG Compression. However, in this comment, we demonstrate that Kumar et al.'s RDH scheme is not robust. The contributions of this paper are summarized as follows:

- (1) This paper tests the percentage of bits changed in each bit plane after JPEG compression and finds that JPEG compression will also cause the contents of MSB planes to be damaged.
- (2) This paper investigates Kumar et al.'s RDH scheme and it analyzes the changes in each bit plane and pixel value ordering caused by JPEG compression to show that we can not extract secret data, thus proving that their scheme is not robust.

The rest of the paper is organized as follows. In **Section 2**, Kumar et al.'s RDH scheme is briefly reviewed. Experimental results and analysis are shown in **Section 3**. Finally, the paper is concluded in **Section 4**.

2. Brief description of Kumar et al.'s RDH scheme

For a self-contained discussion, we briefly review Kumar et al.'s RDH scheme and recommend [14] to readers for more detailed information about it.

To facilitate the introduction of the scheme, secret data is denoted as \mathbf{S} and an original image of size $h \times w$ is denoted as \mathbf{I} . The pixel values of \mathbf{I} vary in the range of 0-255. The eight main steps of the embedding scheme are summarized as follows:

Step 1: Divide \mathbf{I} into two parts I_{MSB} and I_{LSB} calculated as

$$P_{i,j} = \sum_{k=n}^7 b_k \times 2^k + \sum_{k=0}^{n-1} b_k \times 2^k, \quad (1)$$

where

$$x_{i,j} = \sum_{k=n}^7 b_k \times 2^k, \quad (2)$$

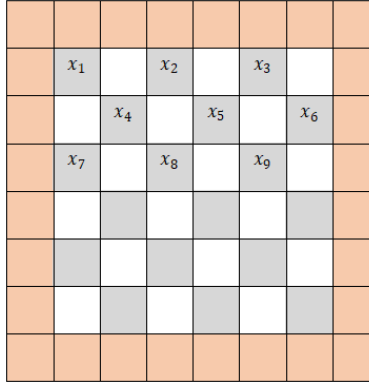
$$l_{i,j} = \sum_{k=0}^{n-1} b_k \times 2^k. \quad (3)$$

$P_{i,j}$ denotes the pixel at the coordinate (i,j) of \mathbf{I} , $x_{i,j}$ represents MSB planes of the pixel, $l_{i,j}$ denotes LSB planes of the pixel and b_k is the bit value in the k -th location, n represents the number of planes of LSB planes, n can vary from 1 to 8.

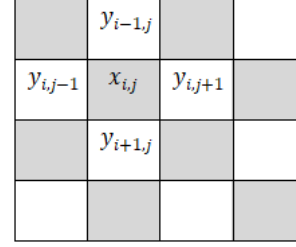
- Step 2: Preprocess I_{HSB} , construct a location map and compress it to achieve a compressed location map.
- Step 3: Save the least significant bit of pixels of I_{MSB} and attach the saved bits and compressed location map to the end of \mathbf{S} .
- Step 4: Make use of the pattern in [Fig.1\(a\)](#) to divide the image as in [14]. Sort the grey pixels based on their local complexity and embed the first part of \mathbf{S} using two-layer embedding in [13]. The local complexity of $x_{i,j}$ is calculated according to variance ($\mu_{i,j}$) of surrounding pixels $(y_{i,j-1}, y_{i-1,j}, y_{i,j+1}, y_{i+1,j})$ (see [Fig.1\(b\)](#)) by

$$\mu_{i,j} = \frac{1}{4} \sum_{t=1}^4 (M_{i,j} - v_t)^2, \quad (4)$$

where $v_t (1 \leq t \leq 4)$ is the ascending sequence of the surrounding pixels, $M_{i,j}$ is the mean value of $v_t (1 \leq t \leq 4)$.



(a) Chessboard representation of image



(b) Prediction pattern. The four surrounding pixels (y_1, y_2, y_3, y_4) are used to measure the local complexity for the pixel x_i , and sorted sequence, (y_1, y_2, y_3, y_4) is used to predict x_i .

Figure 1: Chessboard Pattern and Prediction pattern

Step 5: Arrange the white pixels according to their local complexity and embed the remaining part of \mathbf{S} using two-layer embedding.

Step 6: Combine the resultant MSB planes and LSB planes to obtain the marked image.

Step 7: Repeat Step 4 to Step 6 for all the three predictors, select the most suitable predictor (N) and marked image according to application requirements.

Step 8: Replace the $(n+1)$ -th least significant bit of border pixels of the marked image to save N and the coordinate of the last pixel to embed the secret data (C_{end}) using the least significant bit substitution scheme.

3. Robust testing against JPEG compression

In Step 4 described in Section 2, their scheme used the partition pattern in Fig.1(a) to generate independent cells, then rearranged the grey pixels with ascending order according to local complexity. In this way, secret data can be embedded into pixels with small local complexity to achieve less distortion. To extract the data correctly, the receiver also sorts the pixels on the basis of local complexity and then processes them in order.

3.1. Changes in MSB planes caused by JPEG compression

Kumar et al. [14] showed that embedding secret data in MSB planes can improve the robustness of the scheme as the slight attacks like JPEG compression make modifications in the lower bit planes, so the content of MSB planes are intact. In fact, JPEG compression results in image pixels change not only in LSB planes but also in MSB planes. The experiments were carried out on 8 standard grey-scale images used by Kumar et al. as shown in Fig.2, each of size 512×512 pixels including Lena, Baboon, Jetplane, Peppers, Barbara, Lake, Elaine and Boat.

We perform JPEG compression with different Quality Factors (QF) on the original images. The dissimilarity, between the original image (\mathbf{I}) and the processed image (\mathbf{I}') after JPEG compression, has been observed by the Number Of Bit Change Rate (NBCR). The NBCR indicates the percentage of bits in each bit plane that is changed after JPEG compression. NBCR is formulated as

$$NBCR = \frac{1}{h \times w} \left[\sum_{i=1}^h \sum_{j=1}^w (I_k(i, j) \oplus I'_k(i, j)) \right] \times 100\%, \quad (5)$$

where \oplus represents exclusive-or (XOR) operation, $I_k(i, j)$ and $I'_k(i, j)$ denotes the k -th bit plane of image \mathbf{I} and \mathbf{I}' respectively.

The testing results are shown in Fig. 3, where the horizontal axis represents different QF, the vertical axis represents the average NBCR of eight original images, the 1-st bit plane represents the least significant bit plane and the 8-th bit

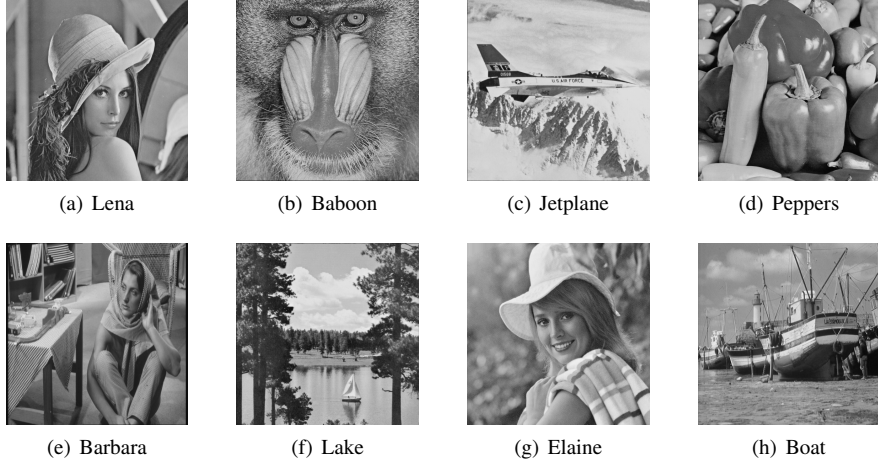


Figure 2: Original images, each of size 512×512 pixels

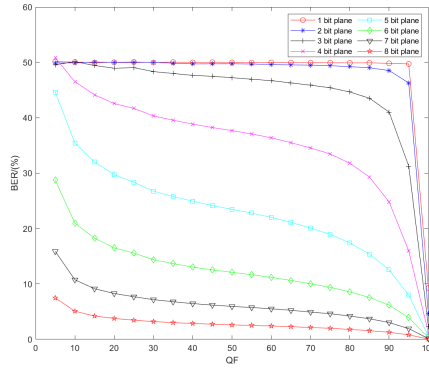


Figure 3: Average NBCR of 8 original images on different bit plane

plane represents the most significant bit plane. We can see that the NBCR of 1-st bit plane reaches about 50% when the quality factor is below 95, which indicates that the least significant bit plane can be easily changed. Among eight bit planes, the 8-th bit plane has the lowest NBCR, which is the most stable. But even at the lowest NBCR, the NBCR is 0.0574%. For each bit plane, as the QF increases, NBCR decreases, which implies that the larger the QF, the fewer bits are modified. Therefore, next we will select QF=100 and QF=95 for further analysis.

In Step 8 described in Section 2, auxiliary information, such as predictor number (N) and the coordinate of the last pixel carrying data (C_{end}), is embedded into $(n+1)$ -th LSB. Here, we set $n = 3$ as an example. From Table 1, the 4-th bit plane where the auxiliary information is embedded has an average NBCR of 1.1526% after JPEG compression under QF = 100. Therefore, auxiliary information can be damaged easily. The average NBCR of MSB and LSB are 0.4437% and 5.4231%, respectively, so neither MSB nor LSB planes are robust. From Table 2, when the compression QF is 95, the average NBCR of the 4-th bit plane has reached 15.9620%. The average NBCR of MSB and LSB reached 6.1207% and 42.4280%, respectively. Obviously, as the compression QF decreases, the possibility of MSB being destroyed increases. So the auxiliary information is more likely to be damaged. With the damaged N, the prediction scheme will be wrong. The length of the extracted data can be significantly wrong due to the damaged C_{end} . Minor modifications will also have a huge impact on the entire scheme, as a result, the receiver will be unable to extract secret data accurately.

3.2. Changes in pixel value order caused by JPEG compression

In addition, in Step 4, before embedding the secret data, the scanned pixels are arranged according to the order of their local complexity (i.e., ascending order). However, according to the calculation formula of local complexity as

Table 1
NBCR in each bit plane after JPEG compression (QF=100)

Bit Plane	8	7	6	5	4	3	2	1
Lena	0.0702	0.1335	0.2872	0.6012	1.1467	2.3182	4.6494	9.2121
Baboon	0.0870	0.1606	0.2853	0.5722	1.1600	2.3518	4.6864	9.2445
Jetplane	0.0244	0.1183	0.2285	0.5699	1.1272	2.3182	4.6581	9.2857
Peppers	0.0401	0.1366	0.3155	0.6081	1.1559	2.3052	4.6494	9.2991
Barbara	0.0496	0.1251	0.3006	0.5993	1.1227	2.2797	4.6474	9.3307
Lake	0.0210	0.1514	0.3185	0.5810	1.1532	2.2892	4.6082	9.2186
Elaine	0.0839	0.1637	0.2968	0.5867	1.1631	2.3140	4.6677	9.2991
Boat	0.0832	0.1217	0.2831	0.5165	1.1917	2.5196	4.7157	9.2869
Average	0.0574	0.1389	0.2894	0.5794	1.1526	2.3370	4.6603	9.2721

Table 2
NBCR in each bit plane after JPEG compression (QF=95)

Bit Plane	8	7	6	5	4	3	2	1
Lena	1.1330	1.9867	3.8849	8.2031	15.6834	30.9162	46.8094	49.9676
Baboon	1.3954	2.7122	4.7249	9.3334	18.7298	36.0718	48.8811	49.8756
Jetplane	0.3490	1.5476	2.5654	6.1642	12.4996	25.2193	41.7076	48.8037
Peppers	0.5638	1.9424	4.7485	9.1179	17.7017	34.4444	48.5249	49.9241
Barbara	0.6072	1.3199	3.2070	6.3507	12.2925	24.3813	41.9697	49.5552
Lake	0.2911	2.2320	4.3751	8.7959	18.0351	34.5795	48.0885	50.0702
Elaine	1.1753	2.1294	3.8651	7.5867	15.3828	30.1125	45.9869	49.5667
Boat	1.0132	1.5816	4.0531	8.1760	17.3714	34.3925	48.3948	50.0286
Average	0.8160	1.9315	3.9280	7.9660	15.9620	31.2647	46.2954	49.7240

111	108	110	111	114	116	119	114
110	110	111	113	113	115	120	114
113	112	111	113	118	118	119	117
110	110	112	114	117	114	117	117
109	104	108	113	113	117	117	114
109	108	115	111	111	115	117	116
112	112	111	117	111	110	114	112
107	112	117	109	114	113	118	115

(a)

13	13	13	13	14	14	14	14	14
13	13	13	14	14	14	14	15	14
14	14	13	14	14	14	14	14	14
13	13	14	14	14	14	14	14	14
13	13	13	14	14	14	14	14	14
13	13	14	13	13	14	14	14	14
13	13	14	13	13	14	14	14	14
14	14	13	14	13	13	14	14	14
13	14	14	13	14	14	14	14	14

(b)

Figure 4: Selected pixel block with size 8×8 from Lena and its corresponding pixel value matrix
(a) Selected pixel block, (b) MSB matrix with $n = 3$

shown in Eq. (4), changes in pixel value will cause errors of the local complexity value, which affect the arrangement order of the pixel. Thus, JPEG compression will cause the secret data cannot be extracted correctly. The experimental results of the pixel sequence sorted by local complexity before and after compression are shown in [Figs. 4-6](#) and [Table 3](#). To demonstrate the change of pixel ordering clearly, we randomly selected an 8×8 pixel block from Lena, as shown in [Fig.4\(a\)](#). The matrix of the selected area is then divided into two parts by Eqs. (2) and (3) namely MSB and LSB matrix under $n = 3$. The MSB matrix is shown in [Fig.4\(b\)](#).

Because the processing of white pixels is similar to that of grey pixels, only grey pixels are taken as an example here to calculate the local complexity and observe the pixel ordering changes before and after compression. To better illustrate the local complexity of each grey pixel, we numbered it as shown in [Fig.5](#).

	A1	B1	A2	B2	A3	B3	
	B4	A4	B5	A5	B6	A6	
	A7	B7	A8	B8	A9	B9	
	B10	A10	B11	A11	B12	A12	
	A13	B13	A14	B14	A15	B15	
	B16	A16	B17	A17	B18	A18	

Figure 5: The pixel number of gray pixels

Original pixel blocks were compressed with different quality factors, e.g., QF=100, 90, 85. Then the compressed pixel blocks are divided into two parts, namely LSB and MSB matrix under $n = 3$. MSB matrixes under different quality factors are shown in [Fig.6](#). The pixels in red boxes in [Fig.6](#) indicate the pixels that have been changed after JPEG compression. We calculated the local complexity of the uncompressed and compressed MSB grey pixels, which is shown in [Table 3](#).

13 13 13 13 14 14 14 14	13 13 13 13 14 14 14 14	13 13 13 13 14 14 14 14
13 13 13 14 14 14 15 14	13 13 13 14 14 14 14 14	13 13 13 14 14 14 14 14
14 14 13 14 14 14 14 14	14 13 14 14 14 14 14 14	13 13 13 14 14 14 14 14
13 13 14 14 14 14 14 14	14 13 14 14 14 14 14 14	13 13 13 14 14 14 14 14
13 13 13 14 14 14 14 14	13 13 13 14 14 14 14 14	13 13 13 14 14 14 14 14
13 13 14 13 14 14 14 14	13 13 13 14 13 14 14 14	13 13 13 14 14 14 14 14
14 14 13 14 14 13 14 14	14 13 14 14 13 14 14 13	13 13 14 14 14 14 14 14
13 14 14 13 14 14 14 14	13 13 14 14 14 14 14 14	13 14 14 13 14 14 14 14

(a)

(b)

(c)

Figure 6: MSB matrix of compressed pixel blocks

(a) QF=100,(b) QF=90,(c) QF=85

We arrange the pixels according to the ascending order of their local complexity. From [Table 3](#), the order of uncompressed pixel block in [Fig. 4\(b\)](#) would be $O = (A5, A8, A9, A12, A16, A1, A3, A4, A10, A14, A18, A2, A13, A15, A17)$. When pixel block is compressed with QF=100 ([Fig. 6\(a\)](#)), it is found that the value of (A17, B14) changes from (13, 13) to (14, 14). As the value of white pixel B14 changes, the local complexity of the surrounding pixels (A11, A14, A15, A17) changes from (0.1875, 0.1875, 0.2500, 0.2500) to (0, 0, 0.1875, 0.1875), which results in a change in pixel ordering. As a result, the order of compressed pixel under QF = 100 is changed to $O_{100} = (A5, A8, A9, A11, A12, A14, A16, A1, A3, A4, A6, A10, A15, A17, A18, A2, A7, A18, A2, A7, A13)$. There only A5, A8, A9 are still in the same place. The order of compressed pixel under QF=90 is changed to $O_{90} = (A1, A3, A5, A6, A8, A9, A12, A11, A15, A17, A18, A4, A7, A10, A14, A16)$. None of the pixels is in their original position. The order of compressed pixel under QF=85 is changed to $O_{85} = (A1, A3, A5, A6, A7, A9, A11, A12, A13, A15, A17, A18, A2,$

Table 3

Change in local complexity of gray pixels because of JPEG compression:(a) gray pixel A1-A9, (b) gray pixel A10-A18

QF	A1	A2	A3	A4	A5	A6	A7	A8	A9
Original	0.1875	0.2500	0.1875	0.1875	0	0.1875	0.2500	0	0
100	0.1875	0.2500	0.1875	0.1875	0	0.1875	0.2500	0	0
90	0.1875	0	0.2500	0	0	0.2500	0	0	0.2500
85	0	0.1875	0	0.1875	0	0	0	0.1875	0

QF	A10	A11	A12	A13	A14	A15	A16	A17	A18
Original	0.1875	0.1875	0	0.2500	0.1875	0.2500	0	0.2500	0.1875
100	0.1875	0	0	0.2500	0	0.1875	0	0.1875	0.1875
90	0.1875	0	0	0.2500	0.1875	0.2500	0.1875	0.1875	0.1875
85	0.1875	0	0	0	0.1875	0	0.2500	0	0

(a)

(b)

A4, A8, A10, A14, A16). As with a QF of 85, all the pixels are out of place. Since JPEG compression causes changes in pixel value, and the local complexity of pixels depends on the pixel value, JPEG compression will lead to errors in the calculation of local complexity, resulting in confusion in pixel ordering. As a result, the secret data extracted by the receiver is grossly inconsistent with the original secret data.

4. Conclusion

In paper "Robust reversible data hiding scheme based on two-layer embedding strategy" published in INS recently, Kumar et al. proposed an RRDH scheme based on two-layer embedding. However, JPEG compression leads to the change of MSB planes, which leads to auxiliary information being damaged, so the length of data extracted by the receiver will be significantly different from the length of the original data. The damaged pixel values caused by JPEG compression change the pixel ordering, so the receiver extracts the secret data in the wrong order. From the above experiments, data cannot be accurately extracted from compressed images, so Kumar et al.'s scheme is not robust.

Declaration of competing interest

This manuscript is the author's original work and has not been published nor has it been submitted simultaneously elsewhere.

Acknowledgements

The authors thank the anonymous referees for their valuable comments and suggestions. This research work is partly supported by National Natural Science Foundation of China (61872003, U20B2068, 61860206004).

References

- [1] Yun-Qing Shi, Xiaolong Li, Xinpeng Zhang, Hao-Tian Wu, and Bin Ma. Reversible data hiding: advances in the past two decades. *IEEE access*, 4:3210–3237, 2016.
- [2] Christophe De Vleeschouwer, J-F Delaigle, and Benoit Macq. Circular interpretation of bijective transformations in lossless watermarking for media asset management. *IEEE Transactions on Multimedia*, 5(1):97–105, 2003.
- [3] Zhicheng Ni, Yun Q Shi, Nirwan Ansari, Wei Su, Qibin Sun, and Xiao Lin. Robust lossless image data hiding designed for semi-fragile image authentication. *IEEE Transactions on circuits and systems for video technology*, 18(4):497–509, 2008.
- [4] Xian-Ting Zeng, Ling-Di Ping, and Xue-Zeng Pan. A lossless robust data hiding scheme. *Pattern Recognition*, 43(4):1656–1667, 2010.
- [5] Xinbo Gao, Lingling An, Yuan Yuan, Dacheng Tao, and Xuelong Li. Lossless data embedding using generalized statistical quantity histogram. *IEEE Transactions on Circuits and Systems for Video Technology*, 21(8):1061–1070, 2011.
- [6] Dekun Zou, Yun Q Shi, Zhicheng Ni, and Wei Su. A semi-fragile lossless digital watermarking scheme based on integer wavelet transform. *IEEE Transactions on Circuits and Systems for Video Technology*, 16(10):1294–1300, 2006.
- [7] Lingling An, Xinbo Gao, Yuan Yuan, Dacheng Tao, Cheng Deng, and Feng Ji. Content-adaptive reliable robust lossless data embedding. *Neurocomputing*, 79:1–11, 2012.

- [8] Lingling An, Xinbo Gao, Xuelong Li, Dacheng Tao, Cheng Deng, and Jie Li. Robust reversible watermarking via clustering and enhanced pixel-wise masking. *IEEE Transactions on image processing*, 21(8):3598–3611, 2012.
- [9] Dinu Coltuc. Towards distortion-free robust image authentication. In *Journal of Physics: Conference Series*, volume 77, page 012005. IOP Publishing, 2007.
- [10] Dinu Coltuc and Jean-Marc Chassery. Distortion-free robust watermarking: a case study. In *Security, Steganography, and Watermarking of Multimedia Contents IX*, volume 6505, page 65051N. International Society for Optics and Photonics, 2007.
- [11] Xiang Wang, Xiaolong Li, and Qingqi Pei. Independent embedding domain based two-stage robust reversible watermarking. *IEEE Transactions on Circuits and Systems for Video Technology*, 30(8):2406–2417, 2019.
- [12] Lizhi Xiong, Xiao Han, Ching-Nung Yang, and Yun-Qing Shi. Robust reversible watermarking in encrypted image with secure multi-party based on lightweight cryptography. *IEEE Transactions on Circuits and Systems for Video Technology*, 2021.
- [13] Weiqing Wang, Junyong Ye, Tongqing Wang, and Weifu Wang. Reversible data hiding scheme based on significant-bit-difference expansion. *IET image processing*, 11(11):1002–1014, 2017.
- [14] Rajeev Kumar and Ki-Hyun Jung. Robust reversible data hiding scheme based on two-layer embedding strategy. *Information Sciences*, 512:96–107, 2020.